I&EC research
Industrial & Engineering Chemistry Research

pubs.acs.org/IECR

Article

Assessment of COSMO-SAC Predictions for Solid−Liquid Equilibrium in Binary Eutectic Systems

Daili Peng,* Ahmad Alhadid,* and Mirjana Minceva

Cite This: *Ind. Eng. Chem. Res.* 2022, 61, 13256−13264

Read Online

ACCESS | Metrics & More | Article Recommendations | Supporting Information

ABSTRACT: As green and sustainable solvents, deep eutectic solvents (DESs) have received wide attention in various fields. Predictions of solid−liquid equilibrium (SLE) make it easier to choose DES constituents from a large pool of potential compounds. The conductor-like screening model for segment activity coefficient (COSMO-SAC) predictions for the SLE of 94 nonsalt and 122 salt-based binary eutectic systems was evaluated in this study. It was found that the COSMO-SAC model can provide satisfactory predictions for the eutectic point of most nonsalt eutectic systems. Similar results were obtained when using the ideal solution model. The salt was represented in salt-based eutectic systems using one of two methods: as an ion pair or as fully dissociated ions. COSMO-SAC predictions for salt-based eutectic systems were unsatisfactory regardless of the salt representation method used. This inaccuracy in predicting SLE in the salt-based eutectic systems is not only due to model limitations but also due to the lack of reliable melting properties for thermally unstable salts.

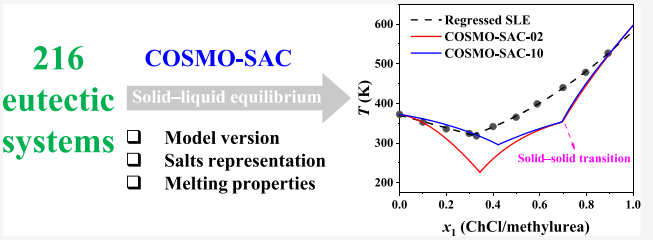

1. INTRODUCTION

In the past few decades, organic solvents have been extensively used in different chemical processes. Meanwhile, researchers gradually recognized their disadvantages, such as high toxicity, volatility, and flammability.[1] With the introduction of the green chemistry concept in recent years, the industry has increased its demand for "greener" solvents for sustainable chemical processes. In this context, alternative solvents such as ionic liquids (ILs),[2,3] supercritical fluids (SFs),[4,5] and deep eutectic systems (DESs)[6,7] have received widespread attention. In comparison to ILs and SFs, DESs have several advantages in terms of toxicity, cost, operating conditions, and equipment requirements.[8] They have been used as solvents in a variety of applications, including extraction,[9,10] gas capture,[11,12] catalysis,[13,14] and battery technology.[15,16]

Eutectic systems (ESs) are mixtures of two or more substances that exhibit partial immiscibility or negligible mutual solubility in the solid phase.[17] With a eutectic temperature (T_e) and composition (x_e), an ES has the lowest possible melting temperature at the eutectic point. Similar to ILs, ESs are also "designer solvents",[7] their thermophysical properties can be customized by proper selection of hydrogen bond acceptors (HBA), hydrogen bond donors (HBD), and their molar ratio. It is critical to understand their solid−liquid equilibrium (SLE) phase diagram before using them as a solvent in a specific process or application. This diagram determines whether the mixture remains liquid at the desired operating temperature. The experimental SLE data are normally obtained by measuring the melting temperature of the mixture at several compositions using visual methods or differential scanning calorimetry (DSC).[18,19] However, given that 10^6−10^8 binary eutectic mixtures could be used as ESs,[20] extensive experimental studies for screening or designing ESs are impractical.[21] As a result, efficient and reliable methods for preselecting ES constituents and tuning their molar ratio were sought.

Several attempts have been made in the literature to model the SLE in binary ESs using correlative thermodynamic models.[22−25] However, because these models rely on experimental SLE data for the determination of their parameters, they can only be applied to a limited number of ESs. Because of its fully predictive nature, the conductor-like screening model for realistic solvation (COSMO-RS) has been applied to predict the SLE of a broader range of ESs.[26] Abranches et al.[27] predicted the SLE diagram for 35 choline chloride (ChCl)-based binary ESs by COSMO-RS. Song et al.[11] developed a method to correlate the melting point depression of ChCl-based ESs using the COSMO-RS molecular descriptors of their HBD. Song et al.[28] evaluated the performance of COSMO-RS for modeling SLE in 118 binary ESs and discovered that the model provides acceptable predictions for T_e but poor predictions for x_e, particularly for

Received: March 13, 2022
Revised: August 13, 2022
Accepted: August 15, 2022
Published: August 24, 2022

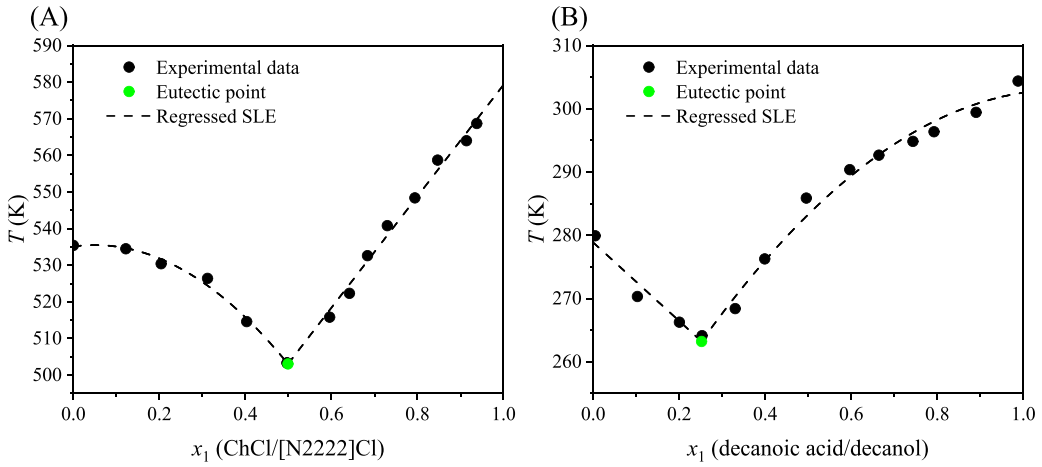

Figure 1. Regressed solid−liquid phase diagram of (A) choline chloride (ChCl)/tetraethylammonium chloride ([N2222]Cl) and (B) decanoic acid/decanol.[44,45]

salt-based systems. In all previous studies, the SLE calculations using COSMO-RS were performed using the COSMOtherm software. Nevertheless, the SLE calculation algorithm implemented in COSMOtherm software is limited to simple ESs containing constituents with no solid−solid transition.[27,28] Although the simple eutectic assumption holds true for the vast majority of reported ESs, cocrystal formation has been observed in a few ESs.[29,30] Furthermore, considering the solid−solid transition in SLE, modeling is inevitable as several ES constituents undergo a solid−solid transition, for example, ChCl,[31] pimelic acid,[32] and borneol.[33]

Based on the COSMO-RS model,[34−36] Lin and Sandler proposed the conductor-like screening model for segment activity coefficient (COSMO-SAC).[37] COSMO-SAC has found wide application in the prediction of vapor−liquid equilibrium or liquid−liquid equilibrium of systems involving organic solvents,[38,39] ILs,[40] and SFs[41] due to its good predictive capabilities for thermodynamic properties. Concerning ES-related studies, more emphasis has been placed on evaluating the performance of the ESs as the solvent (e.g., solubility and selectivity),[42,43] and to the best of our knowledge, there is no comprehensive study concerning the performance of COMO-SAC for the SLE prediction of binary ESs.

In this work, an experimental SLE database containing 216 binary ESs (94 nonsalt and 122 salt-based) was collected from the literature. For salt-based ESs, salts were considered as an ion pair (CA) or fully dissociated ions (C + A). To calculate the eutectic point, two versions of COSMO-SAC and the ideal solution model were used to model SLE in the studied ESs. The SLE calculation took into account the solid−solid transition of pure constituents when applicable. The performance of COSMO-SAC was evaluated based on the deviation of the predicted x_e and T_e from the experimentally observed ones.

2. METHODS

2.1. Experimental SLE Database Collection. A database containing 216 binary ESs (94 nonsalt and 122 salt-based) can be found in Table S1. It should be noted that systems with cocrystal formation were excluded from the database. The eutectic point was determined by fitting the experimental liquidus data for each component to a polynomial function.[27,28] Table S1 contains the degrees of polynomial fit for each system. The x_e and T_e values were determined by calculating the cross point of the fitted liquidus lines as shown in Figure 1.[44,45] The distribution histograms of the acquired x_e and T_e are presented in Figure S1. It was found that 60% of the x_e were located in the range 0.3−0.6, while 49% of the T_e was located in the range 300−350 K.

2.2. SLE Prediction. In this study, only ESs of the simple eutectic type were considered. As a result, the liquidus lines of constituents were calculated by the following equation:[46]

$$\ln(x_i\gamma_i) = \frac{\Delta h_{m,i}}{R}\left(\frac{1}{T_{m,i}} - \frac{1}{T}\right) - \frac{1}{RT}\int_{T_{m,i}}^{T} \Delta c_{p,i}(T)\mathrm{d}T + \int_{T_{m,i}}^{T} \frac{\Delta c_{p,i}(T)}{RT}\mathrm{d}T \quad (1)$$

where γ_i is the activity coefficient of component i at the composition x_i and temperature T; $\Delta h_{m,i}$ and $T_{m,i}$ are the melting enthalpy and temperature of pure component i, respectively; R is the universal gas constant; $\Delta c_{p,i}$ is the change of the molar heat capacity of components i in the liquid and solid states.

Because the last two terms in eq 1 tend to cancel each other when T is not far from $T_{m,i}$ due to their opposite signs,[47] the equation can be simplified to

$$\ln(x_i\gamma_i) = \frac{\Delta h_{m,i}}{R}\left(\frac{1}{T_{m,i}} - \frac{1}{T}\right) \quad (2)$$

When a component undergoes a solid−solid transition, its liquidus line below its solid−solid transition temperature $T_{tr,i}$ can be described as follows:

$$\ln(x_i\gamma_i) = \frac{\Delta h_{m,i}}{R}\left(\frac{1}{T_{m,i}} - \frac{1}{T}\right) + \frac{\Delta h_{tr,i}}{R}\left(\frac{1}{T_{tr,i}} - \frac{1}{T}\right) \quad (3)$$

where $\Delta h_{tr,i}$ is the transition enthalpy.

When considering the ESs as an ideal mixture, unity activity coefficients of components are assumed ($\gamma_i = 1$) in eqs 2 and 3, and the SLE phase diagram and eutectic point of the ESs can be calculated using only the melting and transition properties of the components. The melting properties were gathered from

https://doi.org/10.1021/acs.iecr.2c00856
Ind. Eng. Chem. Res. 2022, 61, 13256−13264

the literature and are listed in Table S2. The melting properties of thermally unstable substances (e.g., ChCl) were mostly estimated in the literature by the ideal solution model using experimental SLE data.[25,44,48,49] Namely, the experimental SLE data were used to regress the $\Delta h_{m,i}$ and/or $T_{m,i}$ with eq 2 for $\gamma_i = 1$. The melting properties obtained on this way are marked in red in Table S2. The same procedure was applied in this work to the substances whose melting properties are unavailable in the literature due to thermal instability, namely, [ACC]Cl, [C3C1pip]Cl, [ClEtMe3N]Cl, [EtNH4]Cl, [NBz,1,1,1]Cl, [N1122OH2]Cl, ChBr, [betaine] HCl, and thenoyltrifluoroacetone. In Table S2, the melting properties of these substances are also highlighted in red. The transition enthalpy and temperature of compounds with a solid−solid transition were mainly obtained from the National Institute of Standards and Technology (NIST) database; data are listed in Table S3.

2.3. COSMO-SAC. Two versions of COSMO-SAC were used to calculate γ_i. The hydrogen bond is described by a cutoff value for the σ-profile in the first version of COSMO-SAC published in 2002 (COSMO-SAC-02).[37] In this version, only the segments having significant charge density differences were assumed to have strong directional attractions with each other. To better describe hydrogen bonding (HB) interactions, a revised version of COSMO-SAC was published in 2010 (COSMO-SAC-10).[50] The molecular surface is divided into segments that cannot form hydrogen bonds (NHB) and segments that can (HB). The HB segments are further subdivided into hydroxyl group hydrogen bonds (OH) and other hydrogen bonds (OT). The OT segments are the surface of nitrogen (N), oxygen (O), fluorine (F), and the hydrogen (H) atoms connected to N and F. Hsieh et al.[51] developed another variant COSMO-SAC model, which takes into account molecule dispersion interactions. Unfortunately, the dispersion parameters of many atoms in ESs (for example, Br, P, and S) are not available. Chen et al.[52] and Chang et al.[53] considered the spatial hydrogen bonding direction in COSMO-SAC. This revised model is more accurate than previous models for many properties. However, the published parameters were optimized using the COSMO files from the Amsterdam Density Functional software. Since a different quantum calculation method was used in this work for calculating COSMO files, this version was left out of the work.

To use COSMO-SAC to calculate the activity coefficient of components in the ESs, their σ-profile should be available. For this purpose, a COSMO file database developed by Xiong et al.[54] was used in this work. The COSMO files for the molecules whose COSMO files were not found in the database were generated by the Dmol3 module in BIOVIA Material Studio (version 2021, San Diego, California, USA) with the VWN-BP functional at the DNP v4.0.0 basis. The detailed descriptions of acquiring the COSMO file can be found in the literature.[54] As described previously, salts can be regarded as an ion pair (CA) or fully dissociated ions (C + A). The C + A method is frequently used in the prediction of thermodynamic properties for IL solutions,[55] whereas the CA method has been reported to improve COSMO-RS prediction of the SLE diagram in ChCl-based ESs.[27] The effect of the representation method of the salt on the performance of COSMO-SAC for the SLE diagram prediction of salt-based ESs was investigated in this study.

3. RESULTS

3.1. Prediction Results for Nonsalt ESs. The predicted x_e and T_e values from the ideal solution and COSMO-SAC models were evaluated simultaneously since the eutectic point contains the information of both the composition and temperature. The predicted eutectic temperature and composition deviation from experimental values for 94 nonsalt ESs is shown in Figure 2. Table S4 lists the predicted x_e and T_e values

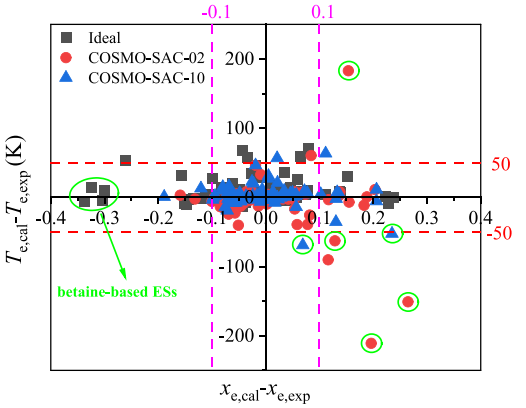

Figure 2. Predicted x_e and T_e deviation from experimental values for nonsalt ESs based on ideal solution, COSMO-SAC-02, and COSMO-SAC-10 models.

for all studied ESs, where x_e is the molar ratio of component 1 in the ESs. As seen in Figure 2, the ideal solution and COSMO-SAC models can provide good predictions for most nonsalt ESs. The numbers of the points, which are located in the region of $-0.1 < x_{e,cal} - x_{e,exp} < 0.1$ and $-50\ \text{K} < T_{e,cal} - T_{e,exp} < 50\ \text{K}$, are 70 for the ideal solution model and COSMO-SAC-10 and 67 for COSMO-SAC-02 according to Table S4. Other researchers also applied the ±50 K criteria for the melting temperature.[28] Table 1 summarizes the COSMO-SAC and ideal solution models' prediction results for x_e and T_e. It should be noted that in some ESs, the predicted x_e is very close to 0 or 1, or the predicted T_e is unreasonably low due to the nearly parallel liquidus lines. In any of the previous cases, the eutectic points were considered unpredicted. It can be seen from Table 1, for the nonsalt ESs, the obtained absolute average deviations (AAD) using the ideal solution model are 0.07 and 10.04 K for x_e and T_e, respectively. Using the ideal solution model, a small deviation between the experimental and calculated eutectic points is observed, indicating that most nonsalt ESs can be regarded as ideal or quasi-ideal mixtures. The AAD of x_e and T_e obtained with COSMO-SAC-10 are very close to those obtained with the ideal solution model. In contrast, COSMO-SAC-02 gives higher deviations than COSMO-SAC-10 and the ideal solution model for the prediction of eutectic temperature ($\text{AAD}_{T_e} = 16.29$ K). In conclusion, COSMO-SAC does not provide significant advantages or provide worse predictions than the ideal solution model for the SLE diagram prediction of nonsalt ESs.

$$\text{AAD} = \frac{\sum_{i=1}^{N} |X_{i,\text{cal}} - X_{i,\text{exp}}|}{N}$$

where $X_{i,cal}$ and $X_{i,exp}$ are the calculated and experimental value of the ES i, respectively; N is the total data points.

https://doi.org/10.1021/acs.iecr.2c00856
Ind. Eng. Chem. Res. 2022, 61, 13256−13264

Table 1. Summary of the Prediction Results of Ideal Solution and COSMO-SAC Models for x_e and T_e

	nonsalt ESs				salt-based ESs					overall			
models	total systems	predicted systems	AAD_{x_e}	AAD_{T_e} (K)	salt representation	total systems	predicted systems	AAD_{x_e}	AAD_{T_e} (K)	total systems	predicted systems	AAD_{x_e}	AAD_{T_e} (K)
ideal	94	94	0.07	10.04		122	111	0.15	30.08	216	205	0.11	20.89
COSMO-SAC-02	94	83	0.06	16.29	CA	122	58	0.11	55.63	216	141	0.08	32.47
					C + A	122	54	0.14	65.01	216	137	0.09	35.49
COSMO-SAC-10	94	83	0.06	9.40	CA	122	72	0.14	46.25	216	155	0.09	26.51
					C + A	122	79	0.15	33.38	216	162	0.10	21.10

As shown in Figure 2, the ideal solution and COSMO-SAC models could not correctly estimate the eutectic point of betaine-based ESs (marked by green circles in Figure 2). The ideal solution accurately predicts the eutectic temperature of betaine-based ESs, but it underestimates the eutectic composition. The COSMO-SAC model, on the other hand, fails to predict the eutectic point of all betaine-based ESs. The erroneous prediction of the eutectic point of betaine-based ESs could be attributed to betaine's melting properties being uncertain. Because betaine is thermally unstable, its melting temperature was calculated using the group contribution method.[56] The uncertainty concerning the melting properties of betaine can strongly influence the prediction of the eutectic point for the corresponding ESs.

3.2. Prediction Results for Salt-Based ESs. The ideal solution and COSMO-SAC models were used to predict the eutectic point of 122 salt-based ESs. Figure 3 shows the predicted eutectic temperature and composition deviation from experimental values. As can be seen, the observed deviation is more dispersed than those of nonsalt ESs (Figure 2). According to Table 1, the deviation obtained using the ideal solution model is lower than those of both COSMO-SAC versions. This does not necessarily imply that the systems are ideal or quasi-ideal. As shown in Figure 3, the ideal solution model overestimates the eutectic temperature of most ESs, which is expected as a substantial negative deviation from ideality is always observed in salt-based ESs. COSMO-SAC-10 also tends to overestimate T_e, while COSMO-SAC-02 underestimates it. Furthermore, both versions of COSMO-SAC poorly predict the SLE for ESs containing polycarboxylic acids, fatty alcohols, and polyols; the eutectic points of these systems are often unpredictable or incorrectly predicted. Similar results were also found when using COSMO-RS.[28] As shown in Table 1, the ideal solution model, when compared to COSMO-SAC, can predict the eutectic point of more salt-based ESs with less deviation, particularly for the T_e. The ideal solution model provides better results because the melting properties of thermally unstable salts were regressed in the literature or this work (available in Table S2) from the available experimental SLE data using the ideal solution model.

As shown in Figure 3, salt representation also influences the prediction results of the COSMO-SAC model. To directly demonstrate the difference between using CA or C + A methods, the σ-profiles of ChCl and [N1111]Cl calculated using these two methods are shown in Figure 4. The σ-profile can be used to identify the ability of a solvent to donate or accept hydrogen bonds. The width and height of the σ-profile curve reflect the polarity distribution of a molecule. Accordingly, the σ-profile is usually divided into HBD, neutral, and HBA zones using the H-bond cutoff values ($\pm$0.0084 e/Å^2).[42] It can be seen that compared to the C + A method, the σ-profile calculated by the CA method is closer to the neutral zone, and less area of their σ-profile is located in the HBD and HBA zones. The main reason for this is that treating the salts as ion pairs increases the number of interacting segments, which offsets the screen charge. As a result, when using the CA method in COSMO-SAC, the corresponding ESs exhibit less-negative deviation from ideality.

Since the calculated σ-profiles are different, the CA and C + A methods also lead to different activity coefficients and SLE diagrams. The CA method provides better predictions for COSMO-SAC-02, as it has been shown in the literature for COSMO-RS.[27] The COSMO-SAC-02 with CA method tends

https://doi.org/10.1021/acs.iecr.2c00856
Ind. Eng. Chem. Res. 2022, 61, 13256−13264

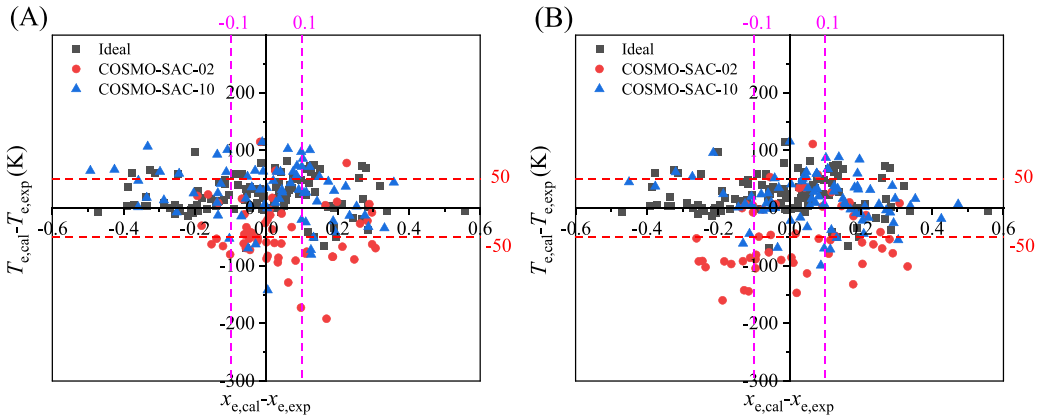

Figure 3. Predicted x_e and T_e deviation from experimental values for salt-based ESs based on (A) CA and (B) C + A methods.

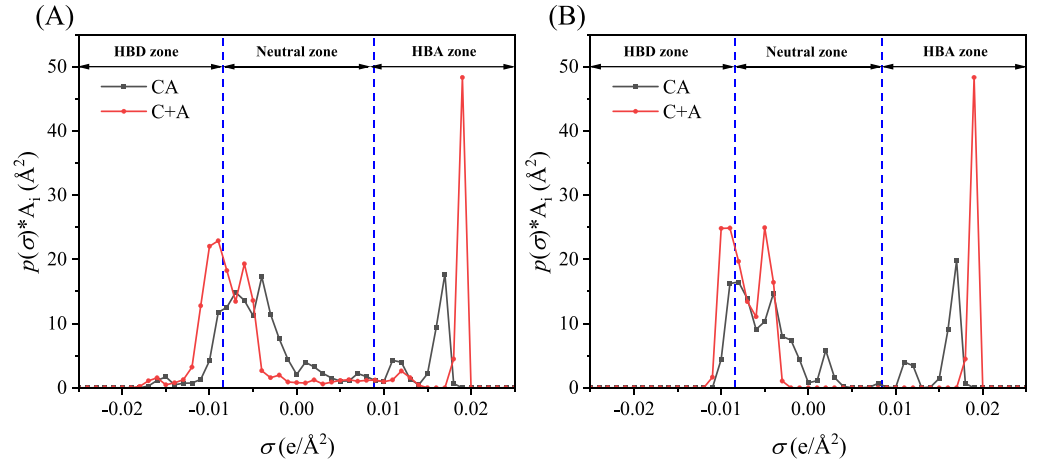

Figure 4. σ-profiles of (A) ChCl and (B) [N1111]Cl calculated by CA and C + A methods.

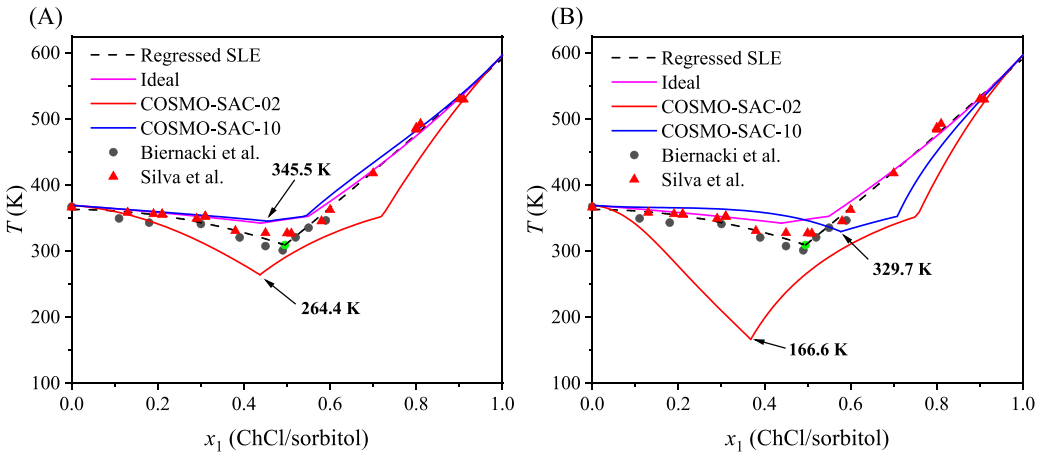

Figure 5. Solid−liquid phase diagram of choline chloride (ChCl)/sorbitol calculated using (A) CA and (B) C + A methods.[8,57]

to underestimate the T_e of salt-based ESs, as illustrated in Figure 3A. According to the results from Figure 4, when the C + A method is used, the negative deviation from ideality of the constituents is overestimated, which tends to reduce the calculated γ_i. As shown in eqs 2 and 3, the low γ_i values can lead to underestimation of T_e. In contrast, the COSMO-SAC-10 with CA method tends to overestimate T_e as seen from Figure 3A. Since the C + A method predicts lower $T_{e,cal}$, it is observed that applying the C + A method in COSMO-SAC-10 leads to better results. An example is given in Figure 5 where the $T_{e,cal}$ in ChCl/sorbitol based on CA and C + A methods are compared.[8,57] It can be seen that the $T_{e,cal}$ of ChCl/sorbitol decreases from 264.4 to 166.6 K when using COSMO-SAC-02 and from 345.5 to 329.7 K when using COSMO-SAC-10.

4. DISCUSSION

The evaluation of COSMO-SAC for the prediction of eutectic points of 216 binary ESs reveals that the COSMO-SAC model provides predictions that are similar to the ideal solution

https://doi.org/10.1021/acs.iecr.2c00856
Ind. Eng. Chem. Res. 2022, 61, 13256−13264

model. The COSMO-SAC model, in particular for salt-based ESs, was found to be insufficient for making reliable predictions. This is due in part to the fact that COSMO-based models were originally developed for molecular systems, and it may be necessary to extend them by introducing long-range ion−ion interactions[58−61] and salt dissociation[62,63] to adequately describe electrolyte systems. It is worth mentioning that long-range interaction was found to play an important role in activity coefficient calculation for the system containing ILs.[58]

Nevertheless, it is unfair to criticize the COSMO-SAC model for the bad prediction results solely. The lack of reliable melting properties of thermally unstable substances may also contribute significantly to the COSMO-SAC model's prediction deviation. Many salts decompose before melting, making it impossible to determine their melting properties. Thus, the melting properties of thermally unstable substances were determined in the literature indirectly from experimental SLE data and assuming the ideal solution model ($\gamma_i = 1$). However, as reported in the literature,[22,25,30,64−66] in salt-based ESs, a negative deviation from ideality is usually expected. Moreover, the melting properties of pure components and their activity coefficients in the liquid phase are interrelated.[67] As a result, a more reliable method for estimating the melting properties of thermally unstable substances is needed.

The availability and reliability of the experimental SLE data also significantly impact the prediction results. If the solidus temperature is unavailable and the system's SLE data are only measured in a narrow composition range, the course of the liquidus line cannot be well described. In the ChCl/lactic acid ES, for example, only three data points are reported for the liquidus line of lactic acid (Figure 6).[68] As a result, without knowledge of the solidus temperature or additional data points, the predicted liquidus line of lactic acid cannot be validated by experimental data.

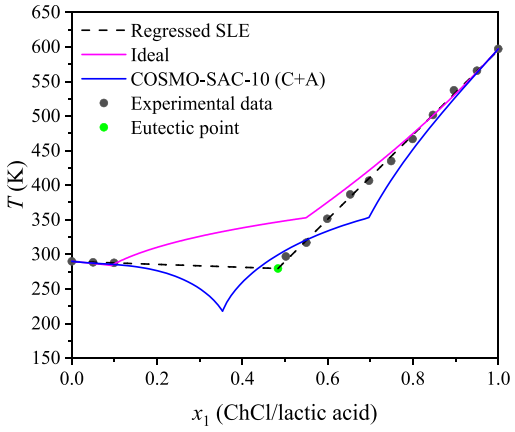

Figure 6. Solid−liquid phase diagram of choline chloride (ChCl)/lactic acid modeled using the ideal solution model and COSMO-SAC-10 (C + A).[68]

Furthermore, many experimental SLE data of ES found in the literature were obtained by visual methods.[45,57,69−71] Although visual methods are simpler to use and provide a direct interpretation of the melting temperature of the mixture, they cannot detect several phase transitions, such as solid−solid or glass transitions. DSC analysis, on the other hand, detects any phase transition in the sample. However, without additional supplementary analysis, such as powder X-ray diffraction, the phase transitions observed in the DSC curves are difficult to interpret. Because most studies solely employed DSC analysis to obtain the SLE data, several phase transitions were perhaps misinterpreted, leading to unreliable estimation of the eutectic point of the ES by the polynomial fit.[29,30,72]

5. CONCLUSIONS

A comprehensive assessment of COSMO-SAC for the SLE prediction of binary ESs based on a database covering 216 binary ESs is presented in this study. Despite the model's simplicity, it was discovered that the phase diagram of most nonsalt ESs can be described by the ideal solution model. The ideal solution model, on the other hand, is insufficient for predicting the SLE of salt-based ESs because a significant negative deviation from ideal behavior frequently occurs. As a result, using the predictive thermodynamic model COSMO-SAC for salt-based ESs is justified. However, most salt-based ESs contain thermally unstable salts, limiting the proper assessment of COSMO-SAC predictions for SLE in these salt-based ESs.

In general, COSMO-SAC-10 gives better prediction results than COSMO-SAC-02. However, both model versions cannot accurately account for the deviation from ideality in the ESs. COSMO-SAC-10 predicts nearly ideal behavior, whereas COSMO-SAC-02 overestimates hydrogen bonding between components. A model extension to describe electrolyte systems may be required to improve the performance of COSMO-SAC for the SLE prediction of salt-based ESs.

The use of predictive thermodynamic models can aid in decreasing the experimental efforts needed to measure the SLE in ES, which is essential for the efficient employing of ESs as solvents in diverse applications. However, the complexity of the SLE phase diagram of some ESs and the absence of their constituents' melting properties limit the reliability of the predictive thermodynamic models in describing the SLE in ESs.

■ ASSOCIATED CONTENT

Supporting Information

The Supporting Information is available free of charge at https://pubs.acs.org/doi/10.1021/acs.iecr.2c00856.

(Table S1) Collected ES database with the regressed eutectic point predictions by polynomial fit, (Table S2) list of the information for all the chemicals involved in the DES database, (Table S3) solid−solid transition properties, (Table S4) comparison of the experimental and predicted x_e and T_e, and (Figure S1) distribution diagram of the experimental x_e and T_e in the database (XLSX)

■ AUTHOR INFORMATION

Corresponding Authors

Daili Peng − *Biothermodynamics, TUM School of Life Sciences, Technical University of Munich, Freising 85354, Germany;* orcid.org/0000-0002-9837-4873; Phone: +49 8161716204; Email: daili.peng@tum.de

Ahmad Alhadid − *Biothermodynamics, TUM School of Life Sciences, Technical University of Munich, Freising 85354, Germany;* orcid.org/0000-0003-1443-1517; Phone: +49 8161716173; Email: ahmad.alhadid@tum.de

https://doi.org/10.1021/acs.iecr.2c00856
Ind. Eng. Chem. Res. 2022, 61, 13256−13264

Author

Mirjana Minceva − *Biothermodynamics, TUM School of Life Sciences, Technical University of Munich, Freising 85354, Germany*

Complete contact information is available at: https://pubs.acs.org/10.1021/acs.iecr.2c00856

Author Contributions

D.P.: conceptualization, methodology, investigations, formal analysis, and writing−original draft; A.A.: conceptualization, formal analysis, and writing−review and editing; and M.M.: supervision and writing−review and editing.

Notes

The authors declare no competing financial interest.

■ ACKNOWLEDGMENTS

This research has received no external funding.

■ NOMENCLATURE AND ABBREVIATIONS

Nomenclature

A_i	cavity surface area of molecular i, Å^2
γ_i	activity coefficient of component i
$\Delta h_{m,i}$	melting enthalpy of component i, J/mol
$\Delta h_{tr,i}$	transition enthalpy of component i, J/mol
$\Delta c_{p,i}$	change of the molar heat capacity of compound i in the liquid and solid phases, J/(K·mol)
N	total data points
R	universal gas constant, 8.3145 J/(K·mol)
T_e	eutectic temperature, K
T	system temperature, K
$T_{m,i}$	melting temperature of component i, K
$T_{tr,i}$	transition temperature of component i, K
σ-profile	screen charge density profile
x_e	eutectic composition
x_i	mole fraction of component i
$X_{i,cal}$	calculated value of i
$X_{i,exp}$	experimental value of i

Abbreviations

AAD	absolute average deviation
COSMO-RS	conductor-like screening model for real solvents
COSMO-SAC	conductor-like screening model for segment activity coefficient
CA	ion pair
C + A	fully dissociated ions
DSC	differential scanning calorimetry
ESs	eutectic solvents
HBA	hydrogen bond acceptors
HBD	hydrogen bond donors
LLE	liquid−liquid equilibrium
NIST	National Institute of Standards and Technology
PC-SAFT	perturbed chain-statistical associating fluid theory
PDH	Pitzer−Debye−Hückel
SLE	solid−liquid equilibria
SFs	supercritical fluids
UNIFAC	universal quasichemical functional-group activity coefficient
VLE	vapor−liquid equilibrium
[ACC]Cl	acetylcholine chloride
[C3C1pip]Cl	1-methyl-1-propylpiperidinium chloride
[ClEtMe3N]Cl	(2-chloroethyl)trimethylammonium chloride
ChCl	choline chloride
ChBr	choline bromide
[EtNH4]Cl	ethylammonium chloride
[NBz,1,1,1]Cl	benzyltrimethylammonium chloride
[N1122OH2]Cl	bis(2-hydroxyethyl)dimethylammonium chloride
[N1111]Cl	tetramethylammonium chloride
[N2222]Cl	tetraethylammonium chloride
[betaine]Cl	betaine hydrochloride

■ REFERENCES

(1) Clarke, C. J.; Tu, W.-C.; Levers, O.; Bröhl, A.; Hallett, J. P. Green and Sustainable Solvents in Chemical Processes. *Chem. Rev.* **2018**, *118*, 747−800.

(2) Wilkes, S. J. A Short History of Ionic Liquids—from Molten Salts to Neoteric Solvents. *Green Chem.* **2002**, *4*, 73−80.

(3) Marija Petkovic, R.; Seddon, K.; Rebelo, L. P. N.; Pereira, C. S. Ionic Liquids: A Pathway to Environmental Acceptability. *Chem. Soc. Rev.* **2011**, *40*, 1383−1403.

(4) Vega, L. F. Perspectives on Molecular Modeling of Supercritical Fluids: From Equations of State to Molecular Simulations. Recent Advances, Remaining Challenges and Opportunities. *J. Supercrit. Fluids* **2018**, *134*, 41−50.

(5) Eckert, C. A.; Knutson, B. L.; Debenedetti, P. G. Supercritical Fluids as Solvents for Chemical and Materials Processing. *Nature* **1996**, *383*, 313−318.

(6) Qin, H.; Hu, X.; Wang, J.; Cheng, H.; Chen, L.; Qi, Z. Overview of Acidic Deep Eutectic Solvents on Synthesis, Properties and Applications. *Green Energy Environ.* **2020**, *5*, 8−21.

(7) Smith, E. L.; Abbott, A. P.; Ryder, K. S. Deep Eutectic Solvents (DESs) and Their Applications. *Chem. Rev.* **2014**, *114*, 11060−11082.

(8) Silva, L. P.; Martins, M. A. R.; Conceição, J. H. F.; Pinho, S. P.; Coutinho, J. A. P. Eutectic Mixtures Based on Polyalcohols as Sustainable Solvents: Screening and Characterization. *ACS Sustainable Chem. Eng.* **2020**, *8*, 15317−15326.

(9) van Osch, D. J. G. P.; Zubeir, L. F.; van den Bruinhorst, A.; Rocha, M. A. A.; Kroon, M. C. Hydrophobic Deep Eutectic Solvents as Water-Immiscible Extractants. *Green Chem.* **2015**, *17*, 4518−4521.

(10) Oliveira, F. S.; Pereiro, A. B.; Rebelo, L. P. N.; Marrucho, I. M. Deep Eutectic Solvents as Extraction Media for Azeotropic Mixtures. *Green Chem.* **2013**, *15*, 1326−1330.

(11) Song, Z.; Hu, X.; Wu, H.; Mei, M.; Linke, S.; Zhou, T.; Qi, Z.; Sundmacher, K. Systematic Screening of Deep Eutectic Solvents as Sustainable Separation Media Exemplified by the CO_2 Capture Process. *ACS Sustainable Chem. Eng.* **2020**, *8*, 8741−8751.

(12) Sarmad, S.; Mikkola, J.-P.; Ji, X. Carbon Dioxide Capture with Ionic Liquids and Deep Eutectic Solvents: A New Generation of Sorbents. *ChemSusChem* **2017**, *10*, 324−352.

(13) Gu, L.; Huang, W.; Tang, S.; Tian, S.; Zhang, X. A Novel Deep Eutectic Solvent for Biodiesel Preparation Using a Homogeneous Base Catalyst. *Chem. Eng. J.* **2015**, *259*, 647−652.

(14) Wang, R.; Qin, H.; Wang, J.; Cheng, H.; Chen, L.; Qi, Z. Reactive Extraction for Intensifying 2-Ethylhexyl Acrylate Synthesis Using Deep Eutectic Solvent [Im:2PTSA]. *Green Energy Environ.* **2021**, *6*, 405−412.

(15) Chakrabarti, M. H.; Mjalli, F. S.; Alnashef, I. M.; Hashim, M. A.; Hussain, M. A.; Bahadori, L.; Low, C. T. J. Prospects of Applying Ionic Liquids and Deep Eutectic Solvents for Renewable Energy Storage by Means of Redox Flow Batteries. *Renewable Sustainable Energy Rev.* **2014**, *30*, 254−270.

(16) Durand, E.; Lecomte, J.; Villeneuve, P. Are Emerging Deep Eutectic Solvents (DES) Relevant for Lipase-Catalyzed Lipophilizations? *OCL: Oilseeds Fats, Crops Lipids* **2015**, *22*, 1−6.

(17) Gamsjäger, H.; Lorimer, J. W.; Scharlin, P.; Shaw, D. G. Glossary of Terms Related to Solubility (IUPAC Recommendations 2008). *Pure Appl. Chem.* **2008**, *80*, 233−276.

(18) Cysewski, P.; Walczak, P.; Ziółkowska, D.; Grela, I.; Przybyłek, M. Experimental and Theoretical Studies on the Sulfamethazine-Urea and Sulfamethizole-Urea Solid-Liquid Equilibria. *J. Drug Delivery Sci. Technol.* **2021**, *61*, 20−22.
(19) Przybyłek, M.; Walczak, P.; Ziółkowska, D.; Grela, I.; Cysewski, P. Studies on the Solid−Liquid Equilibria and Intermolecular Interactions Urea Binary Mixtures with Sulfanilamide and Sulfacetamide. *J. Chem. Thermodyn.* **2021**, *153*, 106308−106320.
(20) Endres, F.; Abbott, A.; MacFarlane, D. *Electrodeposition from Ionic Liquids*; John Wiley & Sons, Ltd., 2017.
(21) Lemaoui, T.; Darwish, A. S.; Attoui, A.; Abu Hatab, F.; Hammoudi, N. E. H.; Benguerba, Y.; Vega, L. F.; Alnashef, I. M. Predicting the Density and Viscosity of Hydrophobic Eutectic Solvents: Towards the Development of Sustainable Solvents. *Green Chem.* **2020**, *22*, 8511−8530.
(22) Kollau, L. J. B. M.; Vis, M.; van den Bruinhorst, A.; de With, G.; Tuinier, R. Activity Modelling of the Solid−Liquid Equilibrium of Deep Eutectic Solvents. *Pure Appl. Chem.* **2019**, *91*, 1341−1349.
(23) Alhadid, A.; Mokrushina, L.; Minceva, M. Design of Deep Eutectic Systems: A Simple Approach for Preselecting Eutectic Mixture Constituents. *Molecules* **2020**, *25*, 1077−1087.
(24) Wolbert, F.; Brandenbusch, C.; Sadowski, G. Selecting Excipients Forming Therapeutic Deep Eutectic Systems—A Mechanistic Approach. *Mol. Pharmaceutics* **2019**, *16*, 3091−3099.
(25) Pontes, P. V. A.; Crespo, E. A.; Martins, M. A. R.; Silva, L. P.; Neves, C. M. S. S.; Maximo, G. J.; Hubinger, M. D.; Batista, E. A. C.; Pinho, S. P.; Coutinho, J. A. P.; Sadowski, G.; Held, C. Measurement and PC-SAFT Modeling of Solid-Liquid Equilibrium of Deep Eutectic Solvents of Quaternary Ammonium Chlorides and Carboxylic Acids. *Fluid Phase Equilib.* **2017**, *448*, 69−80.
(26) Jeliński, T.; Cysewski, P. Application of a Computational Model of Natural Deep Eutectic Solvents Utilizing the COSMO-RS Approach for Screening of Solvents with High Solubility of Rutin. *J. Mol. Model.* **2018**, *24*, 1−17.
(27) Abranches, D. O.; Larriba, M.; Silva, L. P.; Melle-Franco, M.; Palomar, J. F.; Pinho, S. P.; Coutinho, J. A. P. Using COSMO-RS to Design Choline Chloride Pharmaceutical Eutectic Solvents. *Fluid Phase Equilib.* **2019**, *497*, 71−78.
(28) Song, Z.; Wang, J.; Sundmacher, K. Evaluation of COSMO-RS for Solid−Liquid Equilibria Prediction of Binary Eutectic Solvent Systems. *Green Energy Environ.* **2021**, *6*, 371−379.
(29) Alhadid, A.; Mokrushina, L.; Minceva, M. Formation of Glassy Phases and Polymorphism in Deep Eutectic Solvents. *J. Mol. Liq.* **2020**, *314*, 113667−113675.
(30) Alhadid, A.; Jandl, C.; Mokrushina, L.; Minceva, M. Experimental Investigation and Modeling of Cocrystal Formation in L-Menthol/Thymol Eutectic System. *Cryst. Growth Des.* **2021**, *21*, 6083−6091.
(31) Crespo, E. A.; Silva, L. P.; Lloret, J. O.; Carvalho, P. J.; Vega, L. F.; Fèlix Llovell, P.; Coutinho, J. A. A Methodology to Parameterize SAFT-Type Equations of State for Solid Precursors of Deep Eutectic Solvents: The Example of Cholinium Chloride. *Phys. Chem. Chem. Phys.* **2019**, *21*, 15046−15061.
(32) Cingolani, A.; Berchiesi, G. Thermodynamic Properties of Organic Compounds. *J. Therm. Anal.* **1974**, *6*, 87−90.
(33) Chandra, G.; Murthy, S. S. N. Dielectric and Thermodynamic Study of Camphor and Borneol Enantiomers and Their Binary Systems. *Thermochim. Acta* **2018**, *666*, 241−252.
(34) Klamt, A.; Eckert, F. COSMO-RS: A Novel and Efficient Method for the a Priori Prediction of Thermophysical Data of Liquids. *Fluid Phase Equilib.* **2000**, *172*, 43−72.
(35) Klamt, A.; Jonas, V.; Bürger, T.; Lohrenz, J. C. W. Refinement and Parametrization of COSMO-RS. *J. Phys. Chem. A* **1998**, *102*, 5074−5085.
(36) Klamt, A. Conductor-like Screening Model for Real Solvents: A New Approach to the Quantitative Calculation of Solvation Phenomena Starting from the Question of Why Dielectric Continuum Models Give a Fairly Good Description of Molecules. *J. Phys. Chem.* **1995**, *99*, 2224−2235.
(37) Lin, S.-T.; Sandler, S. I. A Priori Phase Equilibrium Prediction from a Segment Contribution Solvation Model. *Ind. Eng. Chem. Res.* **2002**, *41*, 899−913.
(38) Chen, Y.; Zhou, S.; Wang, Y.; Li, L. Screening Solvents to Extract Phenol from Aqueous Solutions by the COSMO-SAC Model and Extraction Process Simulation. *Fluid Phase Equilib.* **2017**, *451*, 12−24.
(39) Fingerhut, R.; Chen, W. L.; Schedemann, A.; Cordes, W.; Rarey, J.; Hsieh, C. M.; Vrabec, J.; Lin, S. T. Comprehensive Assessment of COSMO-SAC Models for Predictions of Fluid-Phase Equilibria. *Ind. Eng. Chem. Res.* **2017**, *56*, 9868−9884.
(40) Yang, J.; Hou, Z.; Wen, G.; Cui, P.; Wang, Y.; Gao, J. A Brief Review of the Prediction of Liquid−Liquid Equilibrium of Ternary Systems Containing Ionic Liquids by the COSMO-SAC Model. *J. Solution Chem.* **2019**, *48*, 1547−1563.
(41) Cai, Z. Z.; Liang, H. H.; Chen, W. L.; Lin, S. T.; Hsieh, C. M. First-Principles Prediction of Solid Solute Solubility in Supercritical Carbon Dioxide Using PR+COSMOSAC EOS. *Fluid Phase Equilib.* **2020**, *522*, 112755−112759.
(42) Verma, R.; Banerjee, T. Liquid−Liquid Extraction of Lower Alcohols Using Menthol-Based Hydrophobic Deep Eutectic Solvent: Experiments and COSMO-SAC Predictions. *Ind. Eng. Chem. Res.* **2018**, *57*, 3371−3381.
(43) Goltz, C.; Barbieri, J. B.; Cavalheiro, F. B.; Toci, A. T.; Farias, F. O.; Mafra, M. R. COSMO-SAC Model Approach for Deep Eutectic Solvent Selection to Extract Quercetin from Macela (A. Satureioides) and Experimental Process Optimization. *Biomass Convers. Biorefin.* **2021**, *1*, 1−10.
(44) Abranches, D. O.; Silva, L. P.; Martins, M. A. R.; Fernandez, L.; Pinho, S. P.; Coutinho, J. A. P. Can Cholinium Chloride Form Eutectic Solvents with Organic Chloride-Based Salts? *Fluid Phase Equilib.* **2019**, *493*, 120−126.
(45) Huang, A.; Deng, W.; Li, X.; Zheng, Q.; Wang, X.; Xiao, Y. Long-Chain Alkanol−Alkyl Carboxylic Acid-Based Low-Viscosity Hydrophobic Deep Eutectic Solvents for One-Pot Extraction of Anthraquinones from Rhei Radix et Rhizoma. *J. Pharm. Anal.* **2022**, *12*, 87−95.
(46) Prausnitz, J.; Lichtenthaler, R. N.; Azevedo, E. G. *Molecular Thermodynamics of Fluid-Phase*; Prentice-Hall, 1999.
(47) Coutinho, J. A. P.; Andersen, S. I.; Stenby, E. H. Evaluation of Activity Coefficient Models in Prediction of Alkane Solid-Liquid Equilibria. *Fluid Phase Equilib.* **1995**, *103*, 23−39.
(48) Kollau, L. J. B. M. *On the Quantification, Description, and Prediction of Eutectic Mixtures*; Technische Universiteit Eindhoven, 2019.
(49) Fernandez, L.; Silva, L. P.; Martins, M. A. R.; Ferreira, O.; Ortega, J.; Pinho, S. P.; Coutinho, J. A. P. Indirect Assessment of the Fusion Properties of Choline Chloride from Solid-Liquid Equilibria Data. *Fluid Phase Equilib.* **2017**, *448*, 9−14.
(50) Hsieh, C.-M.; Sandler, S. I.; Lin, S.-T. Fluid Phase Equilibria Improvements of COSMO-SAC for Vapor−Liquid and Liquid−Liquid Equilibrium Predictions. *Fluid Phase Equilib.* **2010**, *297*, 90−97.
(51) Hsieh, C. M.; Lin, S. T.; Vrabec, J. Considering the Dispersive Interactions in the COSMO-SAC Model for More Accurate Predictions of Fluid Phase Behavior. *Fluid Phase Equilib.* **2014**, *367*, 109−116.
(52) Chen, W.-L.; Lin, S.-T. Explicit Consideration of Spatial Hydrogen Bonding Direction for Activity Coefficient Prediction Based on Implicit Solvation Calculations. *Phys. Chem. Chem. Phys.* **2017**, *19*, 20367−20376.
(53) Chang, C. K.; Chen, W. L.; Wu, D. T.; Lin, S. T. Improved Directional Hydrogen Bonding Interactions for the Prediction of Activity Coefficients with COSMO-SAC. *Ind. Eng. Chem. Res.* **2018**, *57*, 11229−11238.
(54) Xiong, R.; Sandler, S. I.; Burnett, R. I. An Improvement to COSMO-SAC for Predicting Thermodynamic Properties. *Ind. Eng. Chem. Res.* **2014**, *53*, 8265−8278.

https://doi.org/10.1021/acs.iecr.2c00856
Ind. Eng. Chem. Res. 2022, 61, 13256−13264

(55) Yang, L.; Sandler, S. I.; Peng, C.; Liu, H.; Hu, Y. Prediction of the Phase Behavior of Ionic Liquid Solutions. *Ind. Eng. Chem. Res.* **2010**, *49*, 12596−12604.
(56) Jain, A.; Yang, G.; Yalkowsky, S. H. Estimation of Melting Points of Organic Compounds. *Ind. Eng. Chem. Res.* **2004**, *43*, 7618−7621.
(57) Biernacki, K.; Souza, H. K. S.; Almeida, C. M. R.; Magalhães, A. L.; Gonçalves, M. P. Physicochemical Properties of Choline Chloride-Based Deep Eutectic Solvents with Polyols: An Experimental and Theoretical Investigation. *ACS Sustainable Chem. Eng.* **2020**, *8*, 18712−18728.
(58) Chang, C. K.; Lin, S. T. Extended Pitzer-Debye-Hückel Model for Long-Range Interactions in Ionic Liquids. *J. Chem. Eng. Data* **2020**, *65*, 1019−1027.
(59) Müller, S.; González de Castilla, A.; Taeschler, C.; Klein, A.; Smirnova, I. Evaluation and Refinement of the Novel Predictive Electrolyte Model COSMO-RS-ES Based on Solid-Liquid Equilibria of Salts and Gibbs Free Energies of Transfer of Ions. *Fluid Phase Equilib.* **2019**, *483*, 165−174.
(60) Gerlach, T.; Müller, S.; Smirnova, I. Development of a COSMO-RS Based Model for the Calculation of Phase Equilibria in Electrolyte Systems. *AIChE J.* **2018**, *64*, 272−285.
(61) Lee, B. S.; Lin, S. T. Prediction of Phase Behaviors of Ionic Liquids over a Wide Range of Conditions. *Fluid Phase Equilib.* **2013**, *356*, 309−320.
(62) Silva, L. P.; Martins, M. A. R.; Abranches, D. O.; Pinho, S. P.; Coutinho, J. A. P. Solid-Liquid Phase Behavior of Eutectic Solvents Containing Sugar Alcohols. *J. Mol. Liq.* **2021**, *337*, 116392−116400.
(63) Nordness, O.; Brennecke, J. F. Ion Dissociation in Ionic Liquids and Ionic Liquid Solutions. *Chem. Rev.* **2020**, *120*, 12873−12902.
(64) van den Bruinhorst, A.; Kollau, L. J. B. M.; Vis, M.; Hendrix, M. M. R. M.; Meuldijk, J.; Tuinier, R.; Esteves, A. C. C. From a Eutectic Mixture to a Deep Eutectic System via Anion Selection: Glutaric Acid + Tetraethylammonium Halides. *J. Chem. Phys.* **2021**, *155*, No. 014502.
(65) Kollau, L. J. B. M.; Tuinier, R.; Verhaak, J.; Den Doelder, J.; Filot, I. A. W.; Vis, M. Design of Nonideal Eutectic Mixtures Based on Correlations with Molecular Properties. *J. Phys. Chem. B* **2020**, *124*, 5209−5219.
(66) Alhadid, A.; Jandl, C.; Mokrushina, L.; Minceva, M. Cocrystal Formation in Choline Chloride Deep Eutectic Solvents. *Cryst. Growth Des.* **2022**, *22*, 1933−1942.
(67) Alhadid, A.; Mokrushina, L.; Minceva, M. Modeling of Solid−Liquid Equilibria in Deep Eutectic Solvents: A Parameter Study. *Molecules* **2019**, *24*, 2334−2352.
(68) Crespo, E. A.; Silva, L. P.; Martins, M. A. R.; Bülow, M.; Ferreira, O.; Sadowski, G.; Held, C.; Pinho, S. P.; Coutinho, J. A. P. The Role of Polyfunctionality in the Formation of [Ch]Cl-Carboxylic Acid-Based Deep Eutectic Solvents. *Ind. Eng. Chem. Res.* **2018**, *57*, 11195−11209.
(69) Abbott, A. P.; Cullis, P. M.; Gibson, M. J.; Harris, R. C.; Raven, E. Extraction of Glycerol from Biodiesel into a Eutectic Based Ionic Liquid. *Green Chem.* **2007**, *9*, 868−887.
(70) Florindo, C.; Romero, L.; Rintoul, I.; Branco, L. C.; Marrucho, I. M. From Phase Change Materials to Green Solvents: Hydrophobic Low Viscous Fatty Acid-Based Deep Eutectic Solvents. *ACS Sustainable Chem. Eng.* **2018**, *6*, 3888−3895.
(71) Silva, L. P.; Araújo, C. F.; Abranches, D. O.; Melle-Franco, M.; Martins, M. A. R.; Nolasco, M. M.; Ribeiro-Claro, P. J. A.; Pinho, S. P.; Coutinho, J. A. P. What a Difference a Methyl Group Makes−Probing Choline−Urea Molecular Interactions through Urea Structure Modification. *Phys. Chem. Chem. Phys.* **2019**, *21*, 18278−18289.
(72) Abbott, A. P.; Ahmed, E. I.; Prasad, K.; Qader, I. B.; Ryder, K. S. Liquid Pharmaceuticals Formulation by Eutectic Formation. *Fluid Phase Equilib.* **2017**, *448*, 2−8.

https://doi.org/10.1021/acs.iecr.2c00856
Ind. Eng. Chem. Res. 2022, 61, 13256−13264